Published in final edited form as:
Chem Commun (Camb). 2021 October 14; 57(82): 10747–10750. doi:10.1039/d1cc04186j.

Mass spectrometry enables the discovery of inhibitors of an LPS transport assembly *via* disruption of protein–protein interactions†

Francesco Fiorentino[‡,a,b], **Dante Rotili**[c], **Antonello Mai**[c], **Jani R. Bolla**[§,a,b], **Carol V. Robinson**[a]

Antonello Mai: antonello.mai@uniroma1.it; Jani R. Bolla: jani.bolla@chem.ox.ac.uk; Carol V. Robinson: carol.robinson@chem.ox.ac.uk

[a]Physical and Theoretical Chemistry Laboratory, Department of Chemistry, University of Oxford, Oxford, OX1 3QZ, UK

[b]The Kavli Institute for Nanoscience Discovery, 3 South Parks Road, Oxford, OX1 3QU, UK

[c]Department of Drug Chemistry & Technologies, Sapienza University of Rome, P. le A Moro 5, Rome 00185, Italy

[†]Electronic supplementary information (ESI) available. See DOI: 10.1039/ d1cc04186j

[‡]Department of Drug Chemistry and Technologies, Sapienza University of Rome, Rome, Italy

[§]Department of Plant Sciences, University of Oxford, Oxford, OX1 3RB, UK

Abstract

We developed a native mass spectrometry-based approach to quantify the monomer–dimer equilibrium of the LPS transport protein LptH. We use this method to assess the potency and efficacy of an antimicrobial peptide and small molecule disruptors, obtaining new information on their structure–activity relationships. This approach led to the identification of quinoline-based hit compounds representing the basis for the development of novel LPS transport inhibitors.

Recently, the rise of multidrug-resistant bacteria has outpaced the development of new antibiotics, therefore there is an urgent need for new antimicrobial drugs targeting unexplored pathways. Gram-negative bacteria are especially challenging given the presence of a double-membrane envelope. The outer membrane (OM) has an asymmetric arrangement with phospholipids in the inner leaflet and lipopolysaccharide (LPS) in the outer leaflet. LPS is a complex glycolipid forming a tight packing which contributes to OM integrity and impermeability. LPS biosynthesis is executed in the cytoplasm and finalised in the inner membrane (IM) from which it is translocated across the periplasm to the OM through a multiprotein complex.[1] The LPS transport (Lpt) system comprises two membrane subcomplexes. The ABC transporter $LptB_2FGC$ powers LPS extraction from the IM,[2a-c] while LptDE inserts LPS in the outer leaflet of the OM[3a-c] (Fig. 1a). These assemblies are

Conflicts of interest
There are no conflicts to declare.

Europe PMC Funders Author Manuscripts

connected by a periplasmic bridge formed by the oligomeric protein LptA,[4a,b] whose *in vivo* stoichiometry remains under debate.

The presence of LPS in the outer leaflet of the OM is essential for Gram-negative bacteria integrity and cell viability. Disruption of the Lpt system compromises membrane structure, resulting in a highly permeable OM, finally leading to cell death.[5a,b] Hence, targeting OM biogenesis represents a successful strategy for the development of antibacterial drugs. Recent efforts led to the discovery of a diverse range of compounds targeting the Lpt system. These comprise the peptidomimetic compound murepavadin, which binds to *Pseudomonas aeruginosa* LptD,[5b] and the antimicrobial peptide thanatin which interacts with LptD and LptA and disrupts the interaction network between LptC,[6a] LptA, and LptD.[3c,6b] In addition, the quinoline derivative IMB-881, was shown to target LptA and impair LptA–LptC interactions.[6c]

Previous reports indicate that LptA is able to form head-to-tail oligomers. In particular, the *E. coli* LptA has been shown to form concentration-dependent oligomers and has been crystallised as a tetramer.[7a,b] By contrast, LptH, the *P. aeruginosa* orthologue of *E. coli* LptA, exists mainly as a dimer in solution and was crystallised as monomer.[4b] Given the oligomeric nature of LptA/H and the above-mentioned examples of Lpt system-targeting molecules, the most promising approach to inhibit LPS transportation relies on the development of protein–protein interaction (PPI) disruptors targeting LptA/H. These molecules destabilise the periplasmic bridge leading to the release of LptA/H monomers unable to support LPS translocation. Nonetheless, quantitative details regarding LptA/H oligomerisation are not yet available. In addition, further details on known LPS transport inhibitors are necessary to better design new compounds. Indeed, it is not clear whether thanatin targets LptA orthologues from species other than *E. coli*. This is particularly important in the case of *P. aeruginosa* given its rising resistance to established antibiotics.[8] Moreover, the mode of action of the known LPS transport inhibitor IMB-881[6c] requires clarification since there is no experimental evidence on its influence on LptA/H oligomerisation state. Finally, structural modifications are necessary to improve IMB-881 solubility and drug-like properties. To address these points, we have developed a native mass spectrometry (nMS)-based method to probe the oligomeric state of LptH. nMS allows the observation of folded proteins in the gas phase and permits quantitative analysis of subunit stoichiometry and ligand binding.[9a-c] Nonetheless, nMS has not yet been extensively applied to discover PPI disruptors, with relatively few studies reported focussing primarily on known inhibitors.[10] The approach described here enabled us to obtain label-free quantification of protein monomer–dimer equilibrium. In addition, this method allowed to assess the activity of potential drug candidates possessing a diverse range of chemical features in terms of their EC_{50} values and efficacy (E_{max}). Using this platform, we identified novel hit compounds targeting protein dimerisation which serve as scaffolds for further drug design and optimisation of PPI disruptors.

Similar to its *E. coli* orthologue, LptH is folded in a twisted so-called β-taco domain (Fig. 1a, inset). Earlier studies showed the ability of LptH to form dimers[9] and predicted dimerisation sites,[11] however the dissociation constant (K_D) regulating the monomer–dimer equilibrium is currently unknown. This information is pivotal for developing compounds

that act as PPI disruptors. Through nMS we aimed to identify the different LptH oligomerisation states in solution, thereby allowing a quantitative measurement of the K_D.

First, we expressed and purified LptH (ESI:† Methods and Fig. S1) and recorded native mass spectra at increasing LptH concentrations (0.5–60 μM) in a buffer containing 200 mM ammonium acetate (pH 8.0). At each protein concentration, we observed well-resolved charge state distributions corresponding to monomeric and dimeric LptH (Fig. 1b). The experimental masses for the monomer and dimer were 16679.3 ± 0.3 Da and 33359.7 ± 0.6 Da, respectively, in accordance with the theoretical masses (16679.7 Da) and (33359.5 Da). As anticipated, the peak series corresponding to the dimer increases in a concentration-dependent manner, with a concurrent decrease of the monomer charge state series. Measured monomer and dimer populations at different total protein concentration (P_{tot}) were comparable in positive and negative ion modes (Fig. S2, ESI†), indicating that spectral polarity does not influence the monomer/dimer ratio. Plotting the molar fraction of monomer and dimer as a function of total LptH concentration (Fig. 1b, left panel) and fitting we obtain a K_D value for the monomer–dimer equilibrium of 2.45 ± 0.17 μM. We then employed this platform to assess the mode of action of antimicrobial agents that target LPS transport,[9c] by evaluating their influence on monomer–dimer equilibrium. We selected thanatin first (Fig. 1c, upper left panel) since it has been reported to bind to *E. coli* LptA and LptD,[3c,6a,b] but its influence on *P. aeruginosa* Lpt system has not been explored. We incubated LptH (8 μM) with increasing concentrations of thanatin (0–32 μM). Our nMS data indicated perturbation of the monomer–dimer equilibrium even at the lowest concentrations tested with the signal corresponding to the dimer almost abolished even at 4 μM thanatin (Fig. 1c). To quantify thanatin-mediated dimer disruption, we plotted the mole fraction (χ) of monomer and dimer (see ESI†) as a function of thanatin concentration (Fig. 1c, upper right panel). We calculated the concentration at which thanatin exerts half of its maximal dimer disruption effect (EC_{50}) and obtained a value of 1.18 ± 0.15 μM, indicating a strong inhibition of LptH dimer formation. These data indicate that thanatin is a strong inhibitor of LptH dimerisation and exemplify the ability of nMS in capturing compound-mediated modulation of dimer formation.

Another recently discovered LPS transport inhibitor is the quinoline derivative IMB-881 (compound **1a**, Fig. 2a). This molecule has been reported to bind to *E. coli* LptA, preventing its interaction with LptC, thereby blocking LPS transport across the periplasm.[6c] Given its proposed interaction to LptA, we reasoned that it could possess a second mode of action consisting of the disruption of the LptA/LptH oligomer. We incubated LptH (8 μM) with increasing concentrations of **1a** (0–40 μM). Remarkably, **1a** caused a significant increase in the monomer concentration (Fig. 2b). The absence of compound-bound forms is likely a consequence of the weak nature of in-solution interactions between our protein system and the small molecules. Nevertheless, the nMS platform described here was optimised for detection of the pharmacological effect of small-molecule binding, *i.e.* the influence on monomer–dimer equilibrium, rather than binding itself. Analysis of the mole fraction of LptH species as a function of **1a** concentration (Fig. 2c) yielded an EC_{50} value for **1a** of 3.97 ± 0.76 μM. The E_{max} value, expressed as the maximum achievable monomer mole fraction,

was 0.73 ± 0.02, a >2 fold increase of the initial monomer abundance. Together, these data show that **1a** is a potent inhibitor of LptH dimerisation.

We then assessed the activity of **1a** derivatives, in which the phenethyl group on the dihydro-2*H*-[1,3]oxazino nitrogen atom of the prototype was derivatised with different substituents. Compounds **1b** and **1c**, bearing a 3,4-dimethoxyphenethyl and a 2-(cyclohexen-1-yl)ethyl substituents, respectively, displayed EC_{50} values of 50.1 ± 10.5 mM and 22.8 ± 4.2 μM, respectively (Fig. 2d and Fig. S3, Table S1, ESI†). Compounds, **1d, 1e**, and **1f**, possessing shorter spacers and different ring types, were not titrated with LptH since they displayed only a minimal increase (≈20%) in monomer population at 100 μM concentration (Fig. S4, ESI†). These data indicate that the presence of an ethyl spacer is necessary for dimer disruption. In addition, the ring should be unsubstituted and preferentially aromatic. Overall, these results indicate that **1a** is a promising LptH disrupting agent and suggest that the phenethyl group is essential for compound activity.

Although thanatin and **1a** are potent LPS transport inhibitors, they present some drawbacks related to their chemical structure. Indeed, the peptide nature of thanatin makes it prone to rapid renal clearance and metabolic degradation.[12] **1a** has low water solubility (log *P* = 4.54). Very hydrophobic compounds present potential problems in permeating biological membranes, as they may accumulate within the lipid bilayer, and are also prone to extensive liver metabolism.[13] In order to identify molecules with improved drug-like properties, we set out to assess a library of 5-carboxy-8-hydroxyquinoline (IOX-1, **2a**) derivatives bearing a small acyl side chain (**2b–2i**, Fig. 3a). These molecules showed improved water solubility, with log *P* values between 0.71 (**2b**) and 1.81 (**2i**). All compounds share the quinoline core of **1a** and present acyl chains with 4–6 carbon units which may aid interaction with the hydrophobic groove of LptH, which possesses hydrophobic residues that interact with LPS lipid tails. To expand the chemical space of our analysis, we also assayed compound **2j**, which possesses a bulky non-linear substituent on the 5-carboxyamide function (Fig. 3a). When tested at 100 μM, the starting molecule **2a** (IOX-1) exhibited a minimal increase in the monomer mole fraction (Fig. S4, ESI†). Nonetheless, derivatisation at both carboxyl and hydroxyl moieties clearly improved compound activity. Compounds **2b–2e** share a 4-aminobutyric acid residue, which is methylated in **2c** and **2e**, while the 8-hydroxyl function is substituted with a methoxymethyl group in **2d** and **2e**. Among them, compound **2b** displayed low potency (EC_{50} = 42.4 ± 10.3 μM), while compounds **2c, 2d** and **2e** possessed EC_{50} values in the 17–20 μM range (Fig. 3b left panel and Fig. S5, Table S1, ESI†). These data suggest that esterification of the carboxyl acid, as well as substitution of the 8-hydroxyl function, are favourable modifications for activity likely through increased lipophilicity. In addition, **2c** and **2e** showed the highest E_{max} values of the series (Table S1, ESI†), comparable to the value observed for **1a**. These data indicate that the conversion of the carboxylic acid into its methyl ester improves compound activity. Molecules **2f** and **2g**, share a 5-aminovaleric acid chain, which is methylated in the case of **2g**. The addition of an extra carbon to the acyl chain improves potency, as **2f** is ~2 times more potent than **2b**, its butyrate counterpart. Moreover, the esterification of the carboxylic group with methanol increases potency and efficacy, in line with the results obtained with compounds **2c** and **2e** (Fig. S6 and Table S1, ESI†). Molecules **2h** and **2i**, bearing a 5-aminocaproic acid chain, displayed

a decrease in potency, suggesting that the presence of acyl chains >5 carbon atoms may be deleterious for compound activity (Fig. S7 and Table S1, ESI†). Finally, compound **2j**, bearing a bulky *tert*-butyl(2-(4-phenyl)propyl)carbamate, possesses the highest EC_{50} value amongst the **2a** derivatives (Fig. 3b right panel and Fig. S7, ESI†), although its E_{max} is lower than analogues with methylated 4-aminobutyrate and 5-aminovalerate residues (Table S1, ESI†). These data indicate that the presence of a hydrophobic moiety bound to the 5-carboxyamide group increases compound potency but has little effect on efficacy.

The results of this study provide the first quantitative measurement of LptH solution monomer–dimer equilibrium and expand the current knowledge on the peptide thanatin. More generally, we have developed a fast, label-free, and reliable approach to assay small molecule disruptors of protein oligomerisation in a quantitative manner. Our platform allowed us to discover a previously unknown mode of action for **1a** (Fig. 2b and c) and to explore the key moieties necessary for its activity. Focussing on the quinoline core of **1a**, we evaluated a library of compounds bearing different substitutions. We observed that the disruption activity is greater with short acyl chains, up to 5 carbons and protection of carboxyl and hydroxyl groups through methylation and methoxymethylation, respectively, increases compound activity. This may be related to stronger interactions with LptH which presents a large hydrophobic groove that accommodates LPS lipid tails. Given their high potency and simple structure, compounds **2c**, **2e** and **2g** (Fig. 3a) represent ideal hit compounds for further drug development. The hydroxy group at position 8 of the quinoline may be derivatised to resemble the 3-phenethyl-3,4-dihydro-2*H*-[1,3]oxazino moiety of **1a**, pivotal for compound activity.

In conclusion, we developed a method to assess PPI disruptors and yielded valuable hits which may lead to potent inhibitors of LPS transport (Fig. 3c). Disruption of the multi-protein complex impairs LPS transport to the OM with critical consequences for bacterial life. Hence, the development of LptA/LptH oligomerisation inhibitors, starting from the quinoline derivatives presented here, has the potential of providing new therapies to combat multi-drug resistant bacteria.

F. F., J. R. B., and C. V. R. designed the study. F. F. performed the experiments. D. R. and A. M. designed and synthesised compounds **2a–2j**. F. F., J. R. B. and C. V. R. analysed the data and wrote the paper with support from all authors.

C. V. R.’s laboratory is supported by a Medical Research Council (MRC) grant (MR/V028839/1). J. R. B. is researcher co-investigator on the MRC grant. This work was also supported by FISR2019_00374 MeDyCa (A. M.) and Progetto di Ateneo “Sapienza” 2017 no. RM11715C7CA6CE53 (D. R.).

Supplementary Material

Refer to Web version on PubMed Central for supplementary material.

References

1. Lundstedt E, Kahne D, Ruiz N. Chem Rev. 2020; 121: 5098. [PubMed: 32955879]

2. (a) Owens TW, Taylor RJ, Pahil KS, Bertani BR, Ruiz N, Kruse AC, Kahne D. Nature. 2019; 567: 550. [PubMed: 30894747] (b) Li Y, Orlando BJ, Liao M. Nature. 2019; 567: 486. [PubMed: 30894744] (c) Tang X, Chang S, Luo Q, Zhang Z, Qiao W, Xu C, Zhang C, Niu Y, Yang W, Wang T, Zhang Z, et al. Nat Commun. 2019; 10: 4175. [PubMed: 31519889]
3. (a) Qiao S, Luo Q, Zhao Y, Zhang XC, Huang Y. Nature. 2014; 511: 108. [PubMed: 24990751] (b) Dong H, Xiang Q, Gu Y, Wang Z, Paterson NG, Stansfeld PJ, He C, Zhang Y, Wang W, Dong C. Nature. 2014; 511: 52. [PubMed: 24990744] (c) Fiorentino F, Sauer JB, Qiu X, Corey RA, Cassidy CK, Mynors-Wallis B, Mehmood S, Bolla JR, Stansfeld PJ, Robinson CV. Nat Chem Biol. 2021; 17: 187. [PubMed: 33199913]
4. (a) Suits MD, Sperandeo P, Deho G, Polissi A, Jia Z. J Mol Biol. 2008; 380: 476. [PubMed: 18534617] (b) Bollati M, Villa R, Gourlay LJ, Benedet M, Deho G, Polissi A, Barbiroli A, Martorana AM, Sperandeo P, Bolognesi M, Nardini M. FEBS J. 2015; 282: 1980. [PubMed: 25735820]
5. (a) Sperandeo P, Lau FK, Carpentieri A, De Castro C, Molinaro A, Deho G, Silhavy TJ, Polissi A. J Bacteriol. 2008; 190: 4460. [PubMed: 18424520] (b) Srinivas N, Jetter P, Ueberbacher BJ, Werneburg M, Zerbe K, Steinmann J, Van der Meijden B, Bernardini F, Lederer A, Dias RL, Misson PE, et al. Science. 2010; 327: 1010. [PubMed: 20167788]
6. (a) Moura E, Baeta T, Romanelli A, Laguri C, Martorana AM, Erba E, Simorre JP, Sperandeo P, Polissi A. Front Microbiol. 2020; 11: 909. [PubMed: 32477309] (b) Vetterli SU, Zerbe K, Muller M, Urfer M, Mondal M, Wang SY, Moehle K, Zerbe O, Vitale A, Pessi G, Eberl L, et al. Sci Adv. 2018; 4 eaau2634 [PubMed: 30443594] (c) Zhang X, Li Y, Wang W, Zhang J, Lin Y, Hong B, You X, Song D, Wang Y, Jiang J, Si S. Int J Antimicrob Agents. 2019; 53: 442. [PubMed: 30476569]
7. (a) Suits MD, Sperandeo P, Deho G, Polissi A, Jia Z. J Mol Biol. 2008; 380: 476. [PubMed: 18534617] (b) Santambrogio C, Sperandeo P, Villa R, Sobott F, Polissi A, Grandori R. J Am Soc Mass Spectrom. 2013; 24: 1593. [PubMed: 23897621]
8. Willyard C. Nature. 2017; 543: 15. [PubMed: 28252092]
9. (a) Fiorentino F, Bolla JR, Mehmood S, Robinson CV. Structure. 2019; 27: 651. [PubMed: 30799075] (b) Bolla JR, Howes AC, Fiorentino F, Robinson CV. Proc Natl Acad Sci U S A. 2020; 117 17011 [PubMed: 32636271] (c) El-Baba TJ, Lutomski CA, Kantsadi AL, Malla TR, John T, Mikhailov V, Bolla JR, Schofield CJ, Zitzmann N, Vakonakis I, Robinson CV. Angew Chem, Int Ed. 2020; 59 23544
10. Cubrilovic D, Barylyuk K, Hofmann D, Walczak MJ, Gräber M, Berg T, Wider G, Zenobi R. Chem Sci. 2014; 5: 2794.
11. Scala R, Di Matteo A, Coluccia A, Lo Sciuto A, Federici L, Travaglini-Allocatelli C, Visca P, Silvestri R, Imperi F. Sci Rep. 2020; 10 11276 [PubMed: 32647254]
12. Muttenthaler M, King GF, Adams DJ, Alewood PF. Nat Rev Drug Discovery. 2021; 20: 309. [PubMed: 33536635]
13. Waring MJ. Expert Opin Drug Discovery. 2010; 5: 235.

Europe PMC Funders Author Manuscripts

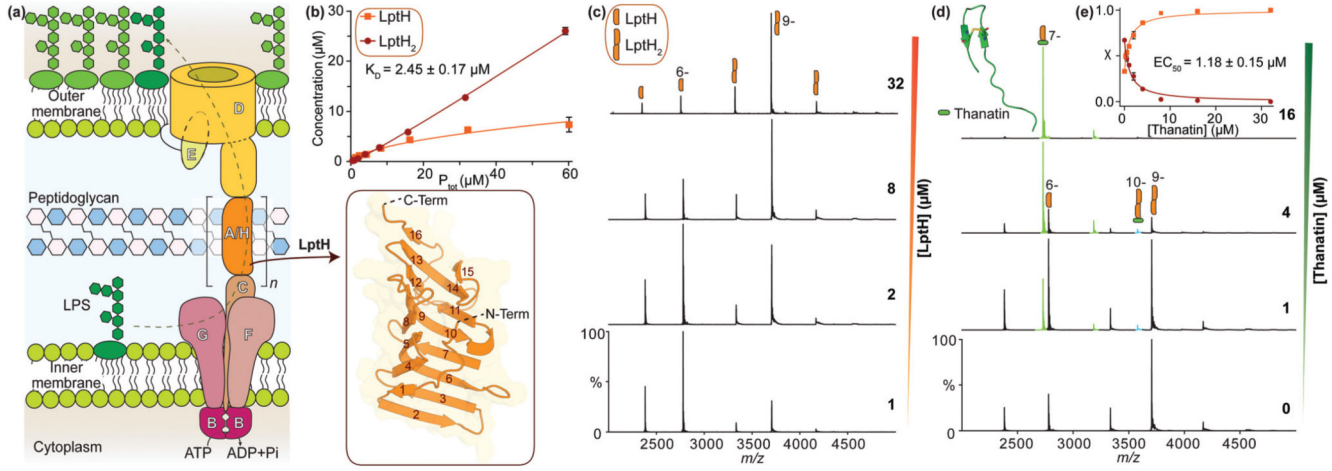

Fig. 1.

(a) Representation of the $LptB_2FG$–$(LptA/H)_n$–LptDE multiprotein complex. Inset: Crystal structure of LptH (PDB ID: 4UU4). (b) Plot of monomer (orange) or dimer (red) concentration as a function of total protein concentration (P_{tot}); the relative mass spectra are shown in (c). (d) Native mass spectra of LptH in the presence of thanatin. Inset: Thanatin solution NMR structure (PDB ID: 5XO4). (e) Plot of monomer (orange) and dimer (red) mole fraction (χ) as a function of thanatin concentration and relative fitting to quantify EC_{50} and E_{max}. Error bars indicate standard deviation (s.d.) ($n = 3$).

Europe PMC Funders Author Manuscripts

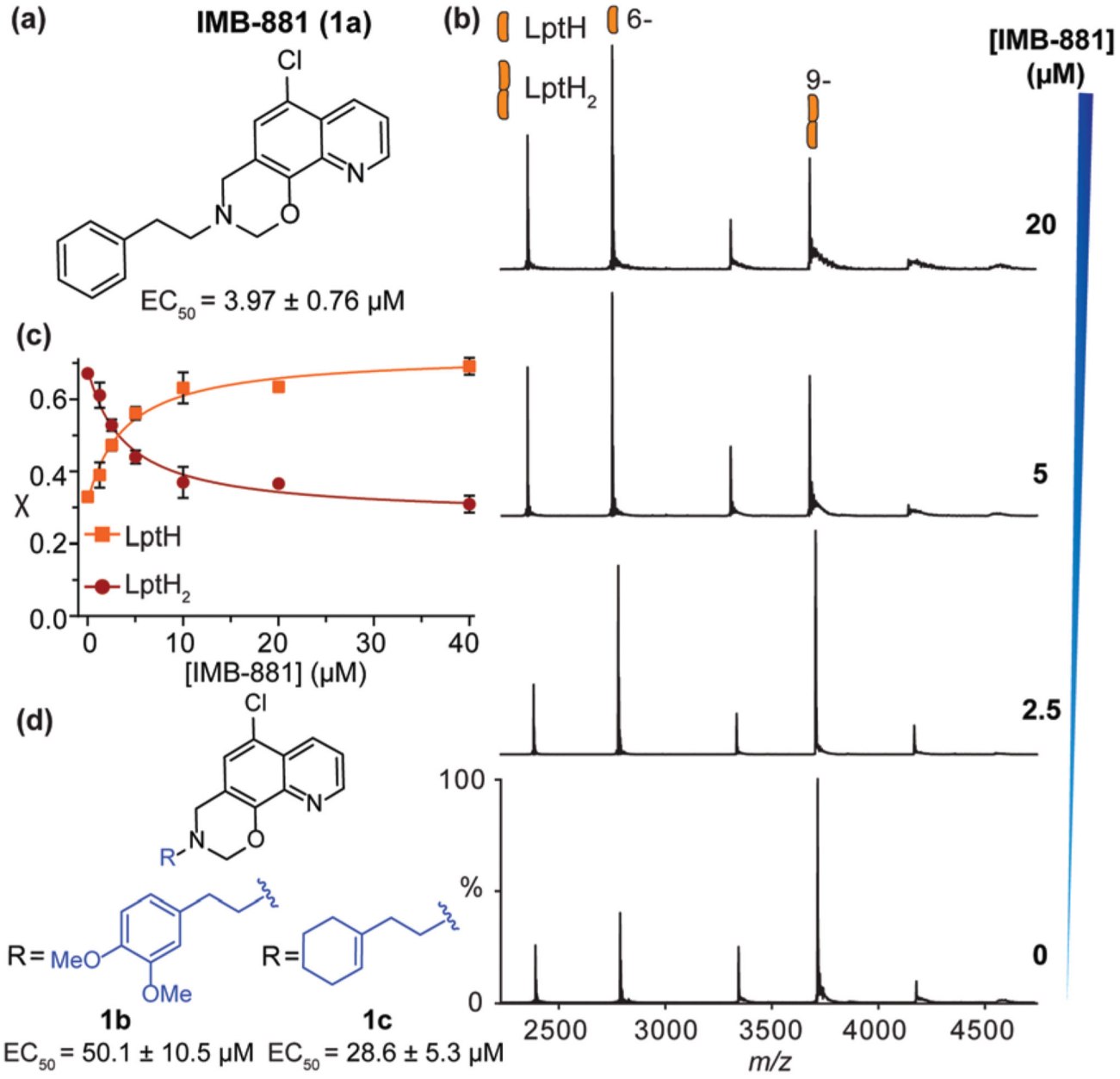

Fig. 2.

(a) Structure and EC_{50} value of IMB-881 (**1a**). (b) Native MS of LptH at increasing concentrations of **1a**. (c) Mole fraction (χ) of LptH monomer and dimer as a function of **1a** concentration. Error bars indicate s.d. ($n = 3$). (d) Structures and EC_{50} values of **1a** derivatives **1b–1c**.

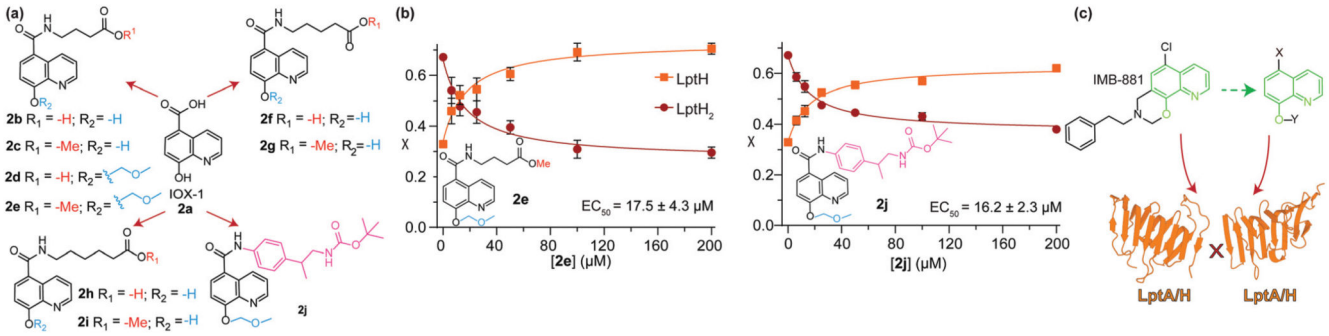

Fig. 3.

(a) Structures of quinoline derivatives employed in this study. (b) Mole fraction (χ) of monomer and dimer as a function of **2e** or **2j** concentration. Error bars indicate s.d. (n = 3). (c) Mode of action and development of quinoline derivatives acting as LptA/H oligomer disruptors.

Europe PMC Funders Author Manuscripts